Structure of proteins under pressure: Covalent binding effects of biliverdin on β-lactoglobulin

Simeon Minić, Burkhard Annighöfer, Arnaud Hélary, Laïla Sago, David Cornu, Annie Brûlet, Sophie Combet

Structure of proteins under pressure: covalent binding effects of biliverdin on β-lactoglobulin

Simeon Minić[1+*], Burkhard Annighöfer[1], Arnaud Hélary[1], Laïla Sago[2], David Cornu[2], Annie Brûlet[1], and Sophie Combet[1*]

[1]Université Paris-Saclay, Laboratoire Léon-Brillouin, UMR12 CEA-CNRS, CEA-Saclay, F-91191 Gif-sur-Yvette CEDEX, France. [2]Université Paris-Saclay, CEA, CNRS, Institute for Integrative Biology of the Cell (I2BC), F-91198 Gif-sur-Yvette CEDEX, France

*Corresponding authors: sophie.combet@cea.fr, simeonminic@yahoo.com

[+]Present address: Center of Excellence for Molecular Food Sciences & Department of Biochemistry, University of Belgrade - Faculty of Chemistry, Belgrade, Serbia.

Running title: BV effects on BLG under pressure

GRAPHICAL ABSTRACT

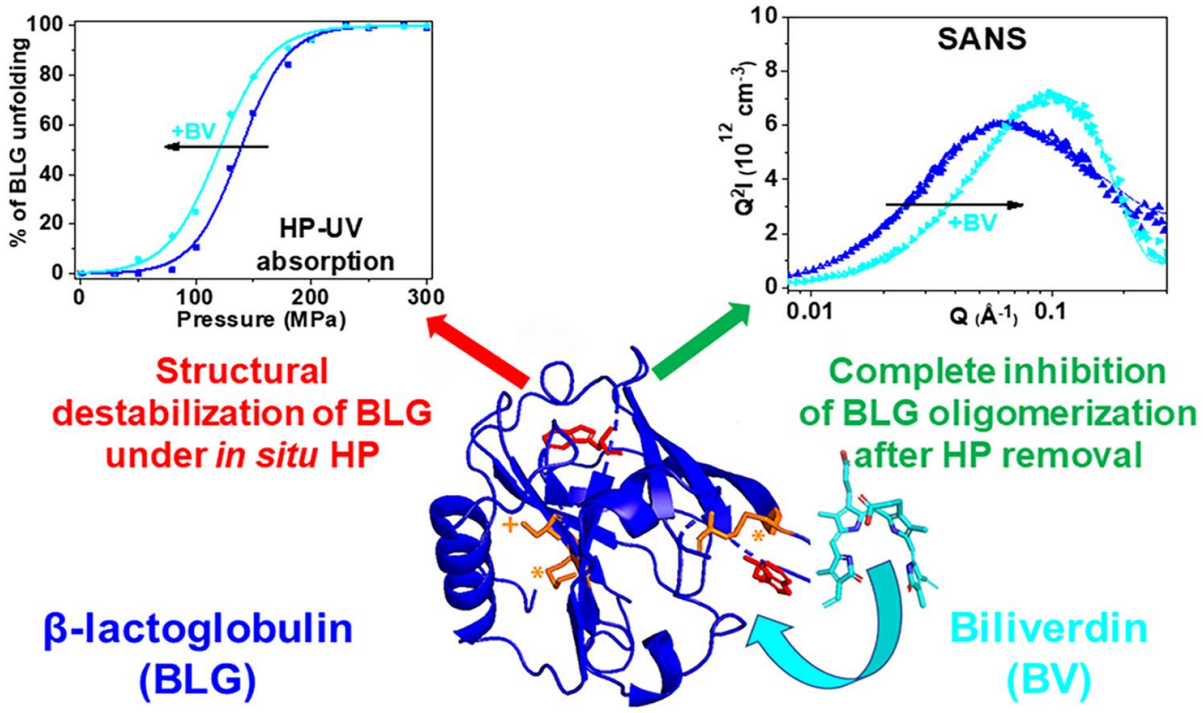

ABSTRACT

High pressure (HP) is a particularly powerful tool to study protein folding/unfolding, revealing subtle structural rearrangements. Bovine β-lactoglobulin (BLG), a protein of interest in food science, exhibits a strong propensity to bind various bioactive molecules. We probed the effects of the binding of biliverdin (BV), a tetrapyrrole linear chromophore, on the stability of BLG under pressure, by combining *in situ* HP-small-angle neutron scattering (SANS) and HP-UV absorption spectroscopy. Although BV induces a slight destabilization of BLG during HP-induced unfolding, a ligand excess strongly prevents BLG oligomerization. Moreover, at SANS resolution, an excess of BV induces the complete recovery of the protein "native" 3D structure after HP removal, despite the presence of the BV covalently bound adduct. Mass spectrometry highlights the crucial role of cysteine residues in the competitive and protective effects of BV during pressure denaturation of BLG through SH/S-S exchange.

STATEMENT OF SIGNIFICANCE

Pressure is a particularly sensitive tool for unfolding proteins and thus better understanding their folding pathway. Bovine β-lactoglobulin (BLG), a protein of interest in food science, has a high propensity to bind various bioactive molecules. We show that biliverdin (BV) completely inhibits BLG oligomerization, making the pressure-induced unfolding of BLG completely reversible. We demonstrated the crucial role of binding to BLG cysteine residues in these protective effects of BV and proposed a disulfide bond exchange mechanism. Added to previous results, this study highlights the effects of various ligands on BLG under pressure as a function of their binding site, their affinity, and their chemical reactivity. Our strategy opens up new possibilities for the structural determination of protein intermediates and oligomers.

INTRODUCTION

High pressure (HP) is a powerful tool to study protein folding/unfolding mechanisms, especially to probe their folding intermediates.[1] It is now well known that the application of HP induces the disruption of the native protein structure due to the decrease of the volume of the protein/solvent system upon denaturation. These pressure-induced structural changes alter the functional properties of the pressurized proteins. Pressure mostly unfolds proteins because the hydrophobic cavities present in the folded state are eliminated in the unfolded states by the water penetration inside.[2] Therefore, ligand binding to the cavities can stabilize proteins and consequently increase their stability under HP.[3]

In food science, HP processing (HPP) has been developed for years on an industrial scale.[4, 5] The advantages of HPP are reduction of energy costs, "greener" processing, and preservation of nutritional values, colours, and flavours.[6-8] This emerging non-thermal technology has shown novel applications in the food industry (texturing, freezing, etc.). In addition, it has been suggested that it allows better protein digestibility.[9] Despite the importance of such macroscopic effects, fundamental studies on HPP, especially concerning *in situ* HP-induced protein structural changes, remain scarce and largely insufficient to establish trends and understand the involved mechanisms.

Bovine β-lactoglobulin (BLG), the major whey protein, exhibits good solubility in a broad pH range, as well as numerous techno-functional properties (such as emulsion stabilization and gel formation), which make it a suitable choice for use as an additive in food industry.[10, 11] However, pressure treatment has detrimental effects on emulsion efficiency and stability of BLG due to its oligomerization and aggregation.[12] Additionally, BLG is one of the most common allergens of milk[13], and the effect of HPP on its allergenicity remains unclear and might strongly depend on the pressure values used.[14]

BLG (Fig. 1) contains a hydrophobic cavity with a strong ability to bind various ligands, as well as a high propensity towards unfolding under HP.[3] From a fundamental point of view, it is a relevant model system to study the effects of ligand binding on protein stability under pressure. BLG belongs to the lipocalin protein family, whose members fold up into eight-stranded antiparallel β-barrels, arranged to form the central hydrophobic cavity. An intramolecular disulfide bridge between the cysteines (Cys) 106 and 119 stabilizes this β-barrel structure. Additionally, Cys66 and Cys160 residues form a second disulfide bond near the edge of the hydrophobic cavity.[15] Finally, Cys121 exists in a free form and is buried under the α-helix located on the surface of the native protein [16] (Fig. 1). Free Cys residues are known to trigger the formation of intermolecular disulfide bonds through SH/S-S interchange reactions under HP or high temperature (HT), leading to the protein covalent oligomerization and/or aggregation.

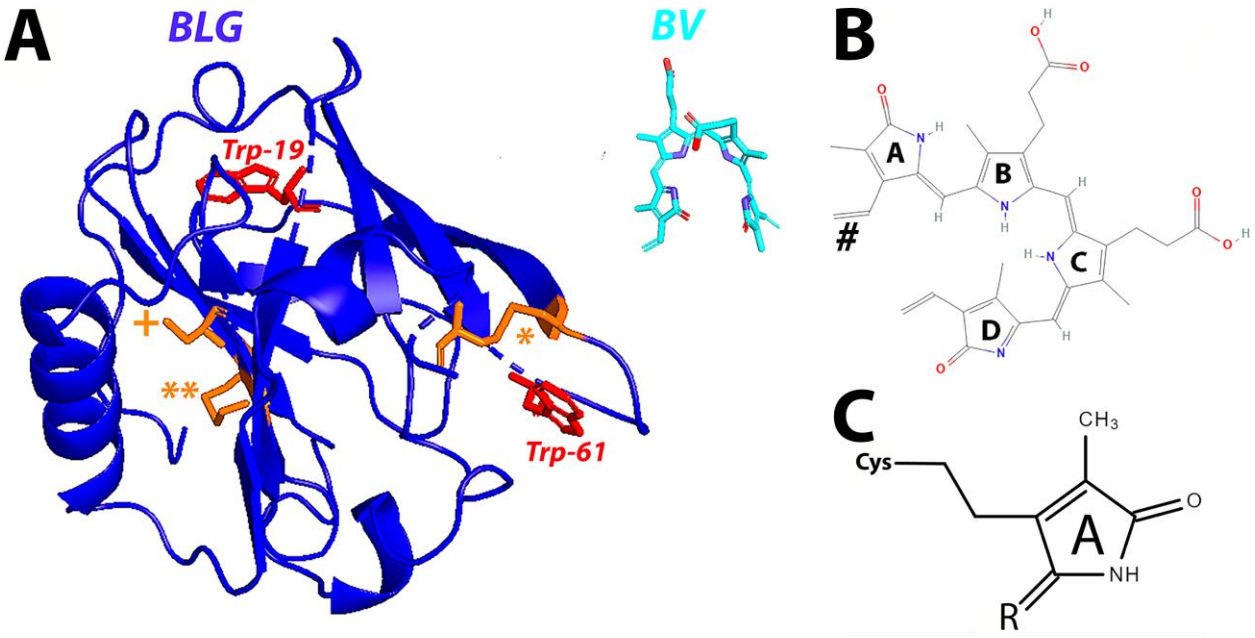

Figure 1. *(**A**) Ribbon model of the crystal structure of BLG monomer (PDB:3BLG). Tryptophan (Trp) aromatic side chains are shown in red (Trp19 and Trp61), with Trp19 residue near the BLG cavity. The two disulfide bridges CyS66-Cys160 (*) and Cys106-Cys119 (**) are shown in orange, as well as the free cysteine Cys121 (+), which is not accessible in the native folded state of BLG but is exposed to the solvent after protein unfolding. The biliverdin (BV) ligand molecule, a tetrapyrrole chromophore, which can react with BLG cysteines, is shown in cyan at the same scale as the protein. (**B**) The chemical formula of BV showing the four (A-D) rings of the ligand. The vinyl side of A ring (marked with #) can react with the free Cys of proteins. (C) Possible structure of BV-BLG adduct, highlighting the covalent bond between the ring A of BV and one Cys residue of BLG. R denotes the rest of BV molecule.*

In our previous *in situ* HP small-angle neutron scattering (HP-SANS) study, we reported that retinol ligand, non-covalently bound to the BLG cavity, can stabilize the protein under HP, but without preventing its irreversible HP-induced unfolding and oligomerization.[3] Besides, modification of BLG free Cys residue by N-ethylmaleimide (NEM) is known to inhibit protein covalent oligomerization at HP or HT conditions,[17] while the cavity conformation is recovered after HP treatment.[18]

Biliverdin (BV) (Fig.1) is a tetrapyrrole chromophore and metabolic product of heme metabolism.[19] Its ability to absorb the longest light wavelength among natural linear tetrapyrrole chromophores makes BV-binding photoreceptors a promising platform for developing optical tools for optogenetic control.[20] The propensity toward covalent binding of BV to Cys residues has been previously proved for phytochromes,[21], as well as *de novo* designed proteins.[22] It is made possible by a single thioether (C–S) bond formed by the nucleophilic attack of Cys residue on the

electrophilic ethylidene side of the ring *A* of BV (Fig. 1, B-C).[23, 24] The different electronic distribution/delocalization and/or steric hindrance of rings *A* and *D* in BV molecule may provide a higher reactivity to ring *A*, as already reported.[21, 24] Besides, it is also very likely that once ring *A* reacts, the reactivity of ring *D* is strongly reduced due to electronic effects and steric hindrance. As a consequence, bridges between two Cys in BLG are very unlikely. Interestingly, besides its potential for covalent binding to proteins, BV may also be reversibly bound to the hydrophobic pocket of apomyoglobin and lipocalin-type prostaglandin D synthase.[25]

Therefore, considering (*i*) the high reactivity of the free SH group within BLG, (*ii*) the propensity of BV for covalent binding to Cys residues, and (*iii*) the fact that the BLG central cavity can accommodate the bile pigment bilirubin and metabolic products of BV,[26] we considered BV as an excellent candidate for binding BLG, covalently or not. The present study aims to characterize such binding and its impact on BLG stability under HP. Using mass spectrometry, we report that BV binds BLG covalently through a Cys residue which, surprisingly, is involved in a disulfide bond in the protein native state. We show that such covalent binding strongly prevents BLG oligomerization after HPP. However, *in situ* measurements highlight that such reversibility is not associated with inhibition of protein unfolding at a multiscale level during pressure increase up to 300 MPa, but rather an unexpected slight destabilization.

MATERIALS & METHODS

Materials. BLG was purified as previously described by Fox *et al.*[27] The protein concentration was determined by spectrophotometry using the extinction coefficient of 17,600 M^{-1} cm^{-1} at 278 nm.[28] BLG was dialyzed against 50 mM Tris buffer in D_2O (pD 7.2 or 8.2) or 100 mM Tris buffer in H_2O (pH 7.2 or 8.2) for HP-SANS or HP-UV absorption measurements, respectively. BV was purchased from Sigma Aldrich (USA) and solubilized in deuterated DMSO (d6, Sigma Aldrich) with concentrations not exceeding 5% (*v*/*v*). All other chemicals were of analytical reagent grade, and milli-*Q* water was used as a solvent.

SDS-PAGE. SDS-PAG electrophoresis of BLG, in absence or presence of BV, before and after HP or HT treatments, was performed under non-reducing conditions[29] unless otherwise stated. A 12 µg of each protein sample was applied on 4-20% gradient precast gel (BioRad, USA). Gels were incubated in 500 mM $ZnCl_2$ for 10 minutes, and bands were visualized under a UV lamp. Then, gels were stained using Coomassie Bradford blue (CBB) G-250 (Sigma Aldrich).

Mass spectrometry (MS). Mass spectrometry measurements were performed with an electrospray triple time-of-flight (TOF) 4600 mass spectrometer (ABSciex) coupled to the nanoRSLC ultra-performance liquid chromatography system (Thermo Scientific) equipped with a C4-desalting column. For electrospray ionization (ESI)−MS measurements, the instrument was operated in positive and radio frequency quadrupole modes, with the TOF data being collected between *m*/*z* 400−2990. The collision energy was set to 10 eV, and azote was used as collision gas. Mass spectra acquisition was performed after loading and desalting of protein samples on the C4 column. The Analyst and Peakview software were used for acquisition and data processing, respectively. Mass spectra were deconvoluted using the MaxEnt algorithm. The protein average masses are calculated from the spectra with a mass accuracy of ± 1 Da.

NanoLC-MSMS peptide analysis. BLG samples were digested before submission to mass spectrometry analysis. Trypsin-generated peptides from BLG isoforms were analyzed by nanoLC-MSMS using a nanoElute liquid chromatography system (Bruker) coupled to a time-of-flight (TOF) Pro mass spectrometer (Bruker). Peptides were loaded with solvent *A* on a trap column (nanoEase C18, 100 Å, 5 µm, 180 µm x 20 mm) and separated on an Aurora analytical column (Ion Optik, 25 cm x 75 µm, C18, 1.6 µm) with a gradient of 0-35% of solvent *B* for 30 min. Solvent *A* was 0.1 % formic acid and 2% acetonitrile in water and solvent *B* was acetonitrile with 0.1% formic acid. MS and MS/MS spectra were recorded from m/z 100 to 1700, with a mobility scan range from 0.6 to 1.4 V.s/cm^2. They were acquired with the PASEF (parallel accumulation serial fragmentation) ion mobility-based acquisition mode, using a number of PASEF MS/MS scans set as 10. MS and MSMS raw data were processed and converted into .mgf files with DataAnalysis software (Bruker). Peptide identification was performed using the MASCOT search engine (Matrix Science, London, UK) against BLG isoforms sequences. Database searches were performed using trypsin cleavage specificity with two possible missed cleavages. BV-Cys mass adduct of 580.23 Da and oxidation of methionines were set as variable modifications. Peptide and fragment tolerances were set at 10 ppm and 0.05 Da, respectively. Only ions with a score higher than the identity threshold and a false-positive discovery rate of less than 1% were considered.

HP-UV absorption spectroscopy. UV absorption spectra at HP conditions were recorded on a Cary 3E spectrometer (Varian, USA) using HP optical bomb with sapphire windows and an HP generator as previously described.[30] A square quartz cell (with an optical pathlength of 5 mm) containing the sample was positioned within the HP optical bomb, while a plastic membrane on the top of the cell separates the sample from the pressure transmitting liquid (H_2O). HP-UV

absorption spectroscopy was performed as previously described[3] with the following slight modifications. UV spectra of BLG solution (100 µM) in the presence or absence of 100 µM BV (BLG-BV 1:1) was recorded between 250 and 310 nm, with a bandwidth of 1 nm and a data interval of 0.02 nm, at a scanning speed of 9 nm/min. Spectra were recorded at various pressures between 0.1 to 300 MPa, with steps of 20 or 30 MPa, at 20°C. The pressure was increased at a rate of 10 MPa/min. After each pressure change, we waited several minutes before starting the measurements to be at the equilibrium. Measurements of buffer solution in the absence or presence of BV (without protein) were performed at the same conditions. The recorded spectra were subtracted from the spectra of BLG without ligand or BLG-BV complexes, respectively. The fourth derivative spectra were calculated by OriginPro 8.5 software (USA) using a Savitzky-Golay smoothing algorithm with 500 points of window. The exact position of the maximum absorption bands at ~291 nm (characteristic of the tryptophan (Trp) residues of BLG) in the fourth derivative spectra was determined. The percentage of protein unfolding as a function of the pressure *P* is calculated using the following equation:

$$\%_{BLG\ unfolding} = \frac{\lambda_{atm} - \lambda_P}{\lambda_{atm} - \lambda_{300MPa}} x100 \qquad \textbf{Eq. 1}$$

where λ_{atm}, $\lambda_{300\ MPa}$, and λ_P represent the absorption maximum at the atmospheric pressure, at 300 MPa, and pressure *P*, respectively. Absorption at 300 MPa is used as a reference of unfolded BLG protein, as shown by Dufour *et al.*[31] The pressure denaturation curves were obtained by expressing the percentage of unfolded BLG as a function of pressure. The apparent Gibbs free energy change ($_{app}\Delta G_{P\,=\,0.1}$ at 0.1 MPa) and the apparent volume change ($_{app}\Delta V_u$) due to unfolding were determined by fitting the pressure denaturation curves with the following equation adapted from Lange et al[32], by replacing the A_l and A_h amplitudes by 0 and 100, respectively.

$$\%_{BLG\ unfolding} = 100 - \frac{100}{1 + e^{-\frac{\Delta G_{P\,=\,0.1} + \Delta V_u * P}{RT}}} \qquad \textbf{Eq. 2}$$

The pressure at which one-half (50%) of proteins is unfolded defines the half denaturation pressure ($P_{1/2}$). The % of unfolding, obtained from Eq. 1, is used to fit the unfolding curves as a function of pressure in Eq. 2, which allows getting both ${}_{app}\Delta G_{P=0.1}$ and ${}_{app}\Delta V_u$.

HP-small-angle neutron scattering (SANS) measurements. SANS measurements were performed on PACE and PAXY SANS instruments at the Laboratoire Léon-Brillouin (LLB, Saclay, France). HP-SANS experiments were performed using a new HP-SANS cell that we developed recently.[33] HP-SANS spectra were recorded for several tens of minutes at 5, 100, 150, 200, 250, and 300 MPa (the pressure change was made also at a rate of 10 MPa/min). Each BLG sample was also measured in a quartz Hellma® cell (with a pathlength of 2 mm) before and after HP treatment. For measurements in a quartz cell, the range of the momentum transfer Q was 5.0 10^{-3}-0.5 $Å^{-1}$, whereas for measurements in the HP cell, due to geometrical and scattering constraints, the Q-range was limited to 2.0 10^{-2}-0.2 $Å^{-1}$, as previously described.[3]

The BLG-BV complex (1:1 molar ratio) was measured at the protein concentration of 8 mg/mL (440 µM) at pD 7.2. The BLG protein without ligand was measured at the same concentration, as a control, in addition with 5% (*v*/*v*) deuterated DMSO. The pressure was increased at a rate of about 10 MPa/min, and the temperature during measurements was kept at 20°C. The pressure dependence for buffer SANS intensity was also checked to be negligible (not shown). A constant incoherent background of 0.05-0.06 cm^{-1}, deduced by measuring the scattering intensity in a Hellma® cell at a Q-range between 0.4 and 0.5 $Å^{-1}$, was subtracted from the SANS intensities of all BLG solutions under pressure. In order to examine the effects of a higher BV concentration (1:4 BLG:BV molar ratio) on the reversibility of BLG unfolding and oligomerization, we performed *ex-situ* SANS measurements (in quartz Hellma® cells), after an HP treatment of 300 MPa during 1 h, at pD 8.2 since BV solubility increases with pH.

Small-angle X-ray scattering (SAXS) measurements. In order to study the effects of BLG:BV molar ratio on HP-induced BLG oligomerization, we performed SAXS measurements on the samples after HP treatment. BLG (440 µM) in the absence or presence of BV (at 440 and 1760 µM, to get 1:1 and 1:4 molar ratios, respectively) was incubated at 300 MPa and pH 8.2 during 1 h. SAXS experiments were carried out on the Xeuss 2.0 apparatus (Xenocs, France) of LLB (SWAXS Lab, CEA-Saclay, France). The instrument uses a micro-focused Cu Kα source (wavelength of 1.54 Å, 8 keV) and a Pilatus3 1M detector (Dectris, Switzerland). Two sample-to-detector distances (SD = 54 or 118 cm) were chosen to cover a *Q*-range extending from 0.01 to 0.1 $Å^{-1}$, with a beam size of 1.2 x 1.2 mm^2 (entrance) or 0.8 × 0.8 mm^2 (exit). Pressurized samples were put in Kapton capillaries. Measurements of buffer (100 mM Tris), empty capillary, empty beam, and electronic background ("dark") were subtracted according to the procedure previously established for SANS.[34] Scattering data normalized to the transmitted X-ray beam and sample thickness (0.145 cm) are in cm^{-1}. Final curves were obtained by the superimposition of the scattering profiles measured at the two different *Q* ranges.

SANS data analysis. The classical expression of the scattering intensity $I(Q)$ (in cm^{-1}) of centro-symmetric, homogenous, and relatively monodisperse particles can be written:

$$I(Q) = n\,\Delta\rho^2\,V_{\text{part.}}^2\;P(Q)\,S(Q) \qquad \textbf{Eq. 3}$$

where n is the number of particles *per* unit volume (cm^{-3}), $\Delta\rho$ (contrast) the difference in the neutron scattering length density between the particles and the solvent (cm^{-2}), and $V_{\text{part.}}$ (cm^3) the specific volume of the particles. The form factor $P(Q)$ describes the shape of the particles and fulfils the condition $P(0) = 1$, while the structure factor $S(Q)$ describes the interactions between the particles. In the absence of interactions, like in a dilute solution, $S(Q) = 1$.

From the scattered intensity $I(0)$, we can extract the mass of the particle in atomic units (MW, in g.mol^{-1}), which coincides with the molecular mass if the particle consists of a single molecule, by introducing the concentration $c = n\frac{MW}{N_A}$ (g.cm^{-3}) and the particle density $d = \frac{MW}{V_{part}.N_A}$ (g.cm^{-3}) using the following equation:

$$MW = \frac{I(0)\, d^2\, N_A}{c\, \Delta\rho^2} \qquad \textbf{Eq. 4}$$

where N_A is the Avogadro number.

The Primus[35] software was used to determine the intensity at zero angle $I(0)$ and the radius of gyration (R_g). These values are defined at small Q-values (QR_g < 0.8-1.4) by the Guinier approximation with[36]:

$$\ln\left(\frac{I(Q)}{I(0)}\right) = -\frac{Q^2 {R_g}^2}{3} \qquad \textbf{Eq. 5}$$

In situ HP-SANS data were fitted with a cylinder model[36] using SasView software (http://www.sasview.org), with obtained χ^2 values not exceeding 1.1. However, the SANS data measured after HP treatment for BLG covalent oligomers were better fitted with a triaxial ellipsoid model[37] with χ^2-values given in Table 3.

BLG covalent oligomers were also estimated by *ab initio* rigid-body modeling (in the Q-range: 0.009–0.5 Å^{-1}), using MASSHA software (ATSAS)[38]. We built oligomers using the crystallographic structure for BLG monomers (PDB:3BLG), as starting building blocks. The previously best-fitted ellipsoid dimensions (SasView) were taken into account to estimate the number and position of the monomers (Fig. 6), which were further adjusted until a satisfactory fit regarding χ^2 (Table 3). To compare with MASSHA results, the number of BLG monomers composing the oligomers was estimated also using, either (*i*) the apparent MW obtained from $I(0)$

in Guinier approximation divided by the monomer *MW* (18.4 kDa), or (*ii*) the ellipsoid or cylinder volume found by fitting in SasView divided by the monomer volume (22 10^3 Å^3, from PDB:3BLG structure) (Table 3).

RESULTS & DISCUSSION

Characterization of BV binding to BLG. We used SDS-PAGE and MS/MS to detect and characterize the covalent binding of BV to BLG (Fig. 2). SDS-PAGE being a denaturing technique, only covalent adducts can be observed. Zn^{2+} ions can bind to BV, and the formed BV/Zn^{2+} complexes exhibit specific fluorescence under a UV light at the same position as the protein bands in the gel (*i.e.* the blue bands on the CBB staining) (Fig. 2A), meaning that BV is covalently bound to BLG. A similar result was obtained for phycocyanobilin (PCB), a BV analogue, in a previous study on BLG.[11] After HP treatment, the covalent BLG-BV adduct is mostly preserved at the monomeric state (Fig. 2A), whereas BLG without ligand is observed at higher *MW* (not shown).

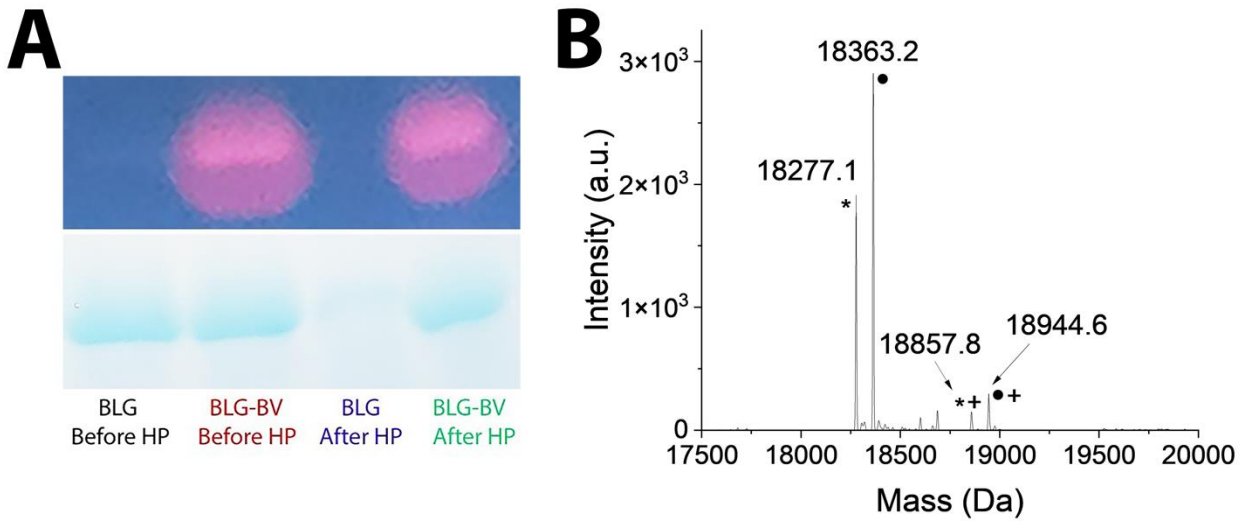

Figure 2. *(**A**) SDS-PAGE at pH 8.2 (in non-reducing conditions) for monomers of unliganded BLG or BLG-BV complex, before and after 300 MPa treatment, for Zn^{2+} visualization (above) or Coomassie Bradford blue (CBB) staining (below). (**B**) Deconvoluted mass spectrum of BLG:BV mixture (molar ratio 1:4), at pH 8.2, after 300 MPa treatment. Peaks with an asterisk or a filled circle correspond to the two known BLG isoforms. A mass increment of 581 Da, corresponding to the covalent binding of one BV to one BLG, is measured for both isoforms (cross).*

A MS/MS spectrum of the BLG-BV reaction mixture is presented in Fig. 2B. In addition to the unmodified BLG isoforms, corresponding covalent BLG-BV adducts are observed, showing that both BLG isoforms are modified to a similar extent. Only one BV molecule is bound *per* BLG protein since the mass of BLG is increased by 581 Da, which corresponds to the mass of one BV molecule (Fig. 2B).

Because of high reactivity of thiols in MS/MS experimental conditions, it is not possible to identify a peptide containing a disulfide bond. It is also very challenging to identify peptides with free cysteines. ESI-MS spectroscopy can detect low abundance peaks arising from BLG-BV adducts but only with gentle ionization conditions. The intensity of the BLG-BV peaks in ESI-MS is much lower in comparison to the peaks of the unmodified proteins (Fig. 2B) and the peak of BV without protein (only ~5% of detected BV are involved in adducts with BLG, see Fig. S2 in Supporting Information). This is not compatible with the complete inhibition of BLG oligomerization we observed by SANS (Fig. 6B) and SDS-PAGE (Fig. 7), as well as the presence of BLG-BV band that is clearly visible on SDS-PAGE by Zn^{2+} fluorescence (Fig. 2A). This strongly suggests that BLG-BV adducts are not stable in the conditions used in MS/MS. To our knowledge, this is the first time that BLG-BV adducts are detected on a protein by this technique, whereas in a previous study, we were able to detect only one fragment of PCB chromophore bound to BLG but not the whole molecule [11].

Cys residues in BLG are known to have a high propensity for covalent binding to small molecules, such as NEM.[17] The reactive Cys121 residue, free in native BLG, can be exposed to the solvent after HP-induced protein unfolding (Fig. 1). Surprisingly, ESI-MS/MS analysis of the peptides, obtained after trypsin digestion of BLG-BV adducts (Fig. S3), demonstrates that BV does not bind to Cys121 but to Cys160, which is not accessible in the native protein but involved in a

disulfide bond (Fig. 1). That reveals SH/S-S interchange reaction within BLG, that have already been observed at high temperature or for the Tanford transition (a conformational change of BLG occurring at around pH 7).[39, 40] Because of disulfide exchange, Cys160 is in the free form and prone to react with BV. We checked the presence of BV-adducts of peptide 102-124 that implies Cys106, Cys119, and Cys121, by performing PMF MALDI-MS analyzes. We managed to identify the peptide 102-124 but only in reduction/alkylation treatment and no differential peak with a BV-adduct mass was observed (not shown). This peptide is not detected in conditions without treatment or with only alkylation. BV chromophore could therefore be partially cleaved during denaturation under acidic conditions (column elution with acetonitrile and formic acid) or during laser ionization, as already reported by Lamparter et al.[21] Therefore, we believe that, during the conditions used for electrospray ionization, BLB-BV adducts are partly degraded, in line with previous observations that spontaneous attachment of tetrapyrroles gives products with low and variable yields due to chromophore instability and propensity to oxidation.[11, 41] We cannot exclude the ability of Cys121 to bind BV, but this adduct is less stable than Cys160-BV. Indeed, a study dealing with BV binding to phytochromes showed that the covalent attachment of BV to Cys residues exhibits different thermodynamic behaviour related to the different environment of the cysteines.[23] Detection of Cys160 may therefore be due to a higher stability and/or reactivity of this residue compared to the other Cys residues of BLG. The latter may be attributed to its localization in the terminal part of the protein, which is more flexible (Fig. 1). Hence, the low stability of adducts at MS conditions does not allow us to make reliable quantification but to give only *qualitative* results by this technique.

Additionally, there is no significant difference in the intensity of the BLG-BV peaks before and after HP treatment, as detected by MS and SDS-PAGE (Figs. S1 and 2A), meaning that

disulfide exchange within BLG is possible even without pressure. However, after extensive dialysis of BLG-BV samples before and after HP, we found by spectrophotometry (at BV absorption at 660 nm) that the relative amount of bound BV is about three times higher after HP treatment than before (not shown). Therefore, although we cannot exclude the formation of covalent adducts before HP treatment, the exposition of the SH group during pressurization is the driving force for additional covalent binding of BV.

Effect of BV on *in situ* HP-induced structural changes of BLG. Depending on pH, temperature, and concentration conditions, BLG can adopt various assembly conformations, *i.e.* monomer, dimer, or octamer structures.[42] Molecular characteristics, scattering length, scattering length density (SLD), and structural parameters of BLG are shown in Table S1. At neutral pH, native BLG (pD 7.2, 8 mg/mL) fits well the crystal structure of dimeric BLG (PDB:1BEB) and can be adjusted by a cylinder form factor, as we previously showed.[3] We checked that the presence of BV ligand does not significantly affect the structural parameters of native BLG (Table 1).

An increase of pD from 7.2 to 8.2 induces a decrease of the protein mass from ~38 to ~29 kDa, due to partial dissociation of dimers into monomers (Table 1), as previously shown by SAXS and SANS studies [3, 43]. However, this *MW* decrease is not associated with R_g modification that remains ~23 Å, which can be explained by opposite effects between the pH-induced partial dissociation of BLG and its higher flexibility at pH 8.2.[43]

Table 1. *Fitting SANS data from BLG samples before HP treatment, using Guinier approximation or cylinder modeling (in SasView software). L and r represent the length and radius of the cylinder, respectively.*

	Guinier approximation			**cylinder modeling**		
Sample	R_g **(Å)**	$I_{Q\to 0}$ **(cm^{-1})**	MW **(kDa)**	L **(Å)**	r **(Å)**	χ^2
BLG (pD 7.2)	23.2 ± 0.5	0.37 ± 0.01	37.9 ± 0.7	81 ± 2	13.9 ± 0.2	1.49
BLG/BV (1:1, pD 7.2)	24.0 ± 0.6	0.39 ± 0.01	40.0 ± 0.8	81 ± 2	14.1 ± 0.1	1.71
BLG (pD 8.2)	23 ± 1	0.28 ± 0.01	28.7 ± 0.5	70 ± 1	13.8 ± 0.2	0.33
BLG/BV (1:4, pD 8.2)	23.2 ± 0.9	0.28 ± 0.01	28.7 ± 0.5	67 ± 1	13.6 ± 0.2	0.31

SANS and UV absorption spectroscopy measurements were performed by applying *in situ* HP up to ~300 MPa on BLG in the presence or absence of BV. For both BLG without ligand and BLG-BV complex, no significant change in the protein 3D conformation is observed by HP-SANS up to ~100 MPa (Fig. 3), except a small decrease of $I_{Q\to 0}$ due both to (*i*) BLG partial dissociation of native dimers into monomers, as similarly observed both by HP-SAXS[44] and HP-SANS[3, 45, 46] under moderate pressures; and (*ii*) to an increase of protein hydration, which reduces the contrast of BLG in D_2O. For such pressures, values of R_g (Fig. 4A), length (Fig. 4C) and radii, derived from the fitted cylinder model of SANS data, decrease slightly compared to those obtained at atmospheric pressure.

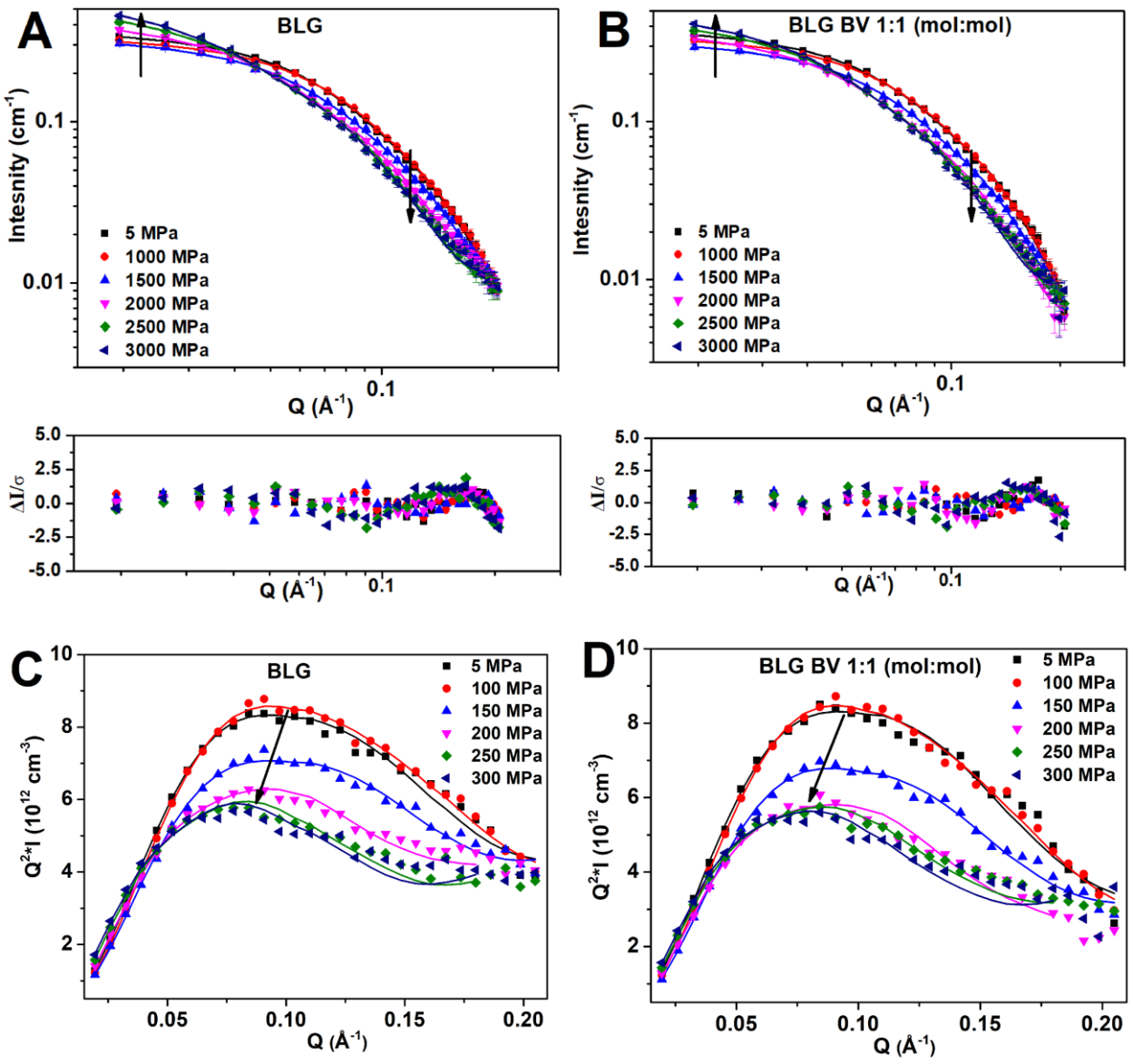

Figure 3. *In situ HP-SANS curves of BLG (8 mg/mL, pD 7.2, 20°C) in absence (**A**) or presence (**B**) of BV ligand (1:1 molar ratio), from atmospheric pressure up to 300 MPa. The full lines represent the best fits to cylinder model. The corresponding error distribution plots are shown below. (**C**, **D**) The same data in Kratky representation.*

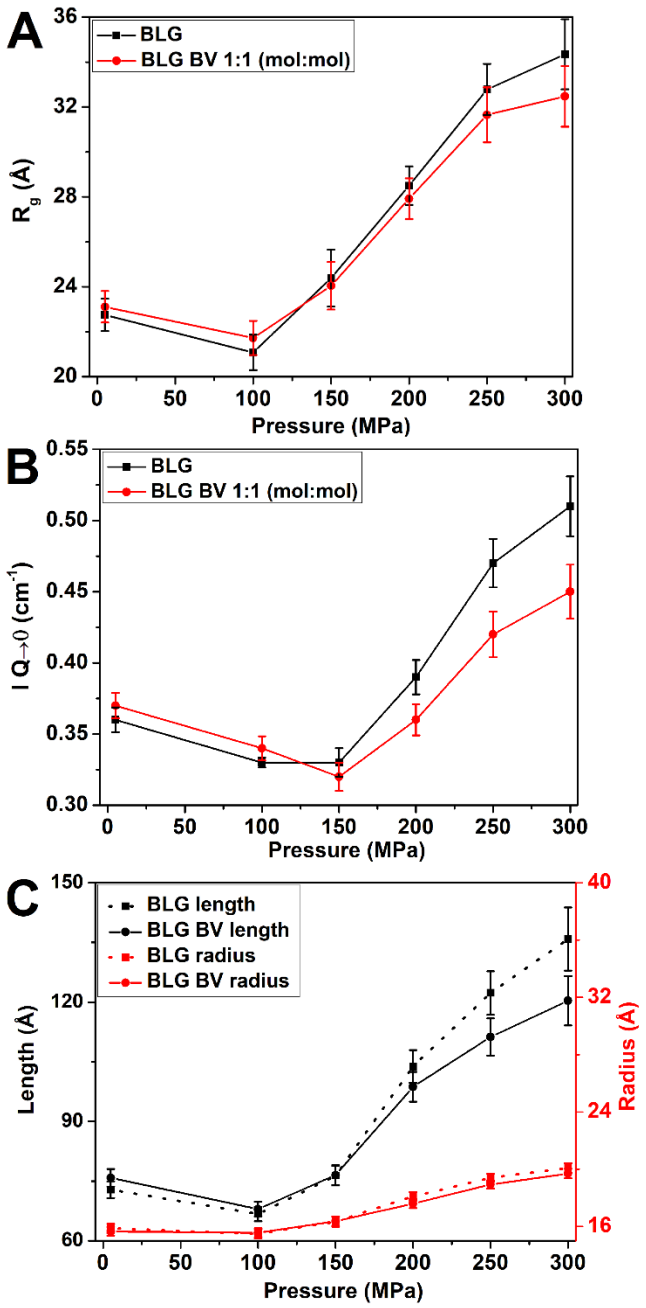

Figure 4. *Pressure dependence of (**A**) R_g and (**B**) $I_{Q\to 0}$ deduced from BLG HP-SANS data (pD 7.2, 8 mg/mL) in absence (squares) or presence (circles) of BV (1:1 molar ratio). (**C**) Evolution, under the same conditions, of the length (circles) and radii (squares) derived from the best fits of the data using a cylinder model, in absence (dotted line) or presence (full line) of BV.*

BLG starts to unfold and oligomerize continuously from ~150 MPa to a "trimeric" state at 250-300 MPa, as shown by the 50% increase of $I_{Q\rightarrow 0}$ value (Fig. 4B) as well as higher R_g values (Fig. 4A). However, at 300 MPa, protein unfolding is not complete since the bell-shaped curves in the Kratky representations (normalized or not) still persist (Fig. 3, C-D, Fig. S1). Therefore, the oligomerization dominates unfolding without preceding it. We observe a clear transition from a globular state at ambient pressure to a more elongated one up to 300 MPa, as shown by the shift of the curve peak to lower *Q*-values (Fig. 3, C-D). Moreover, SANS curves are virtually superimposed both up to ~100 MPa and beyond 200 MPa, whereas, at intermediate pressure (150-200 MPa), the different curves suggest the coexistence of two protein populations depending on their folding state (Fig. 3C). SANS data can be fitted by a cylinder form factor up to ~150 MPa (Fig. 4C). At 200-300 MPa, this model still fits the data, but seems less reliable.

In the presence of BV, the transition process of BLG unfolding is already finished at 200 MPa, Kratky curves at 200-300 MPa being mainly superimposed, strongly suggesting a destabilization effect of the ligand (Fig. 3D). Compared to the unliganded BLG, the transition mentioned above between two protein populations looks sharper in the presence of BV, insofar as only the curve at 150 MPa is separated from the two sets observed at higher and lower pressures. Despite the limited *Q*-range covered by the SANS measurements, it is possible to evaluate the Porod integral, *i.e.* the area under the curves of the Kratky plots, normalized by $I_{Q\rightarrow 0}$, which is inversely proportional to the volume of the oligomers. The ratio of the calculated volumes at low and high pressures is equal to two, confirming that the pressure induces a transition from a state where one and two monomers coexist to a state with three monomers, independently of the fitting of the form factors.

The BV-induced destabilization of BLG may be due to the bulky tetrapyrrole of the ligand, which, by binding to Cys residues, probably induces a slight loss of the tertiary structure of BLG.[11] This was also reported for NEM ligand, which, by blocking Cys residues, induces lower stability of BLG under temperature due to possible steric issues and disruption of non-covalent interactions.[47] Moreover, the observed destabilization of BLG by BV at HP conditions does not support the assumption that BV is bound to the central cavity of protein. Previous *in silico* and *in vitro* studies revealed binding of other tetrapyrrole ligands (PCB and bilirubin) to the hydrophobic cavity of BLG, but without the ability to penetrate deeply into the hydrophobic cavity of native BLG.[11, 26] It is well known that binding of ligands within hydrophobic cavities might stabilize proteins at HP conditions. Indeed, a remarkable increase of BLG stability under pressure was noticed in the presence of retinol (with the shift of $P_{1/2}$ for more than 70 MPa), which is bound in the central cavity of BLG.[3] Moreover, quenching of BLG intrinsic fluorescence by BV is negligible,[25] while cavity-binding ligands such as retinol have a high propensity to quench the fluorescent signal of BLG.[48] Therefore, BV covalent binding to BLG probably occurs somewhere outside of the cavity, preventing the stabilization effect of BV under HP.

As an indicator of protein folding/unfolding, the evolution of R_g may not confirm the destabilization effect of BV (Fig. 4A). Indeed, R_g depends not only on the extent of unfolding but also on the overall size and shape of the molecule. According to the $I_{Q\to 0}$ plots, BV decreases BLG oligomerization at HP conditions (Fig. 4B), leading to smaller oligomer sizes, which also reduce R_g values. Therefore, in the presence of BV at HP conditions, two phenomena are observed: (*i*) destabilization of BLG folding by binding and (*ii*) inhibition of its oligomerization upon unfolding under HP, which oppositely affects R_g variations.

In the HP-UV absorption study, using the 4th derivative mode (Fig. 5, A-B, and Fig. S4), BLG spectra exhibit absorbance maxima at 276, 291, and 284 nm, corresponding to tyrosine (Tyr) or tryptophan (Trp) residues or both of them, respectively (Fig. 5). For all BLG samples, HP treatment induces a "blue shift" of these maxima, especially of the Trp-dependent peak, towards lower wavelengths, indicating a higher polarity of the Trp environment, as a consequence of the movement of the aromatic side chains from the hydrophobic protein environment towards a more hydrated BLG cavity during protein unfolding.[49] This applies particularly to the Trp19 residue, buried inside the hydrophobic cavity of BLG in native condition but exposed to the solvent upon denaturation.[50]

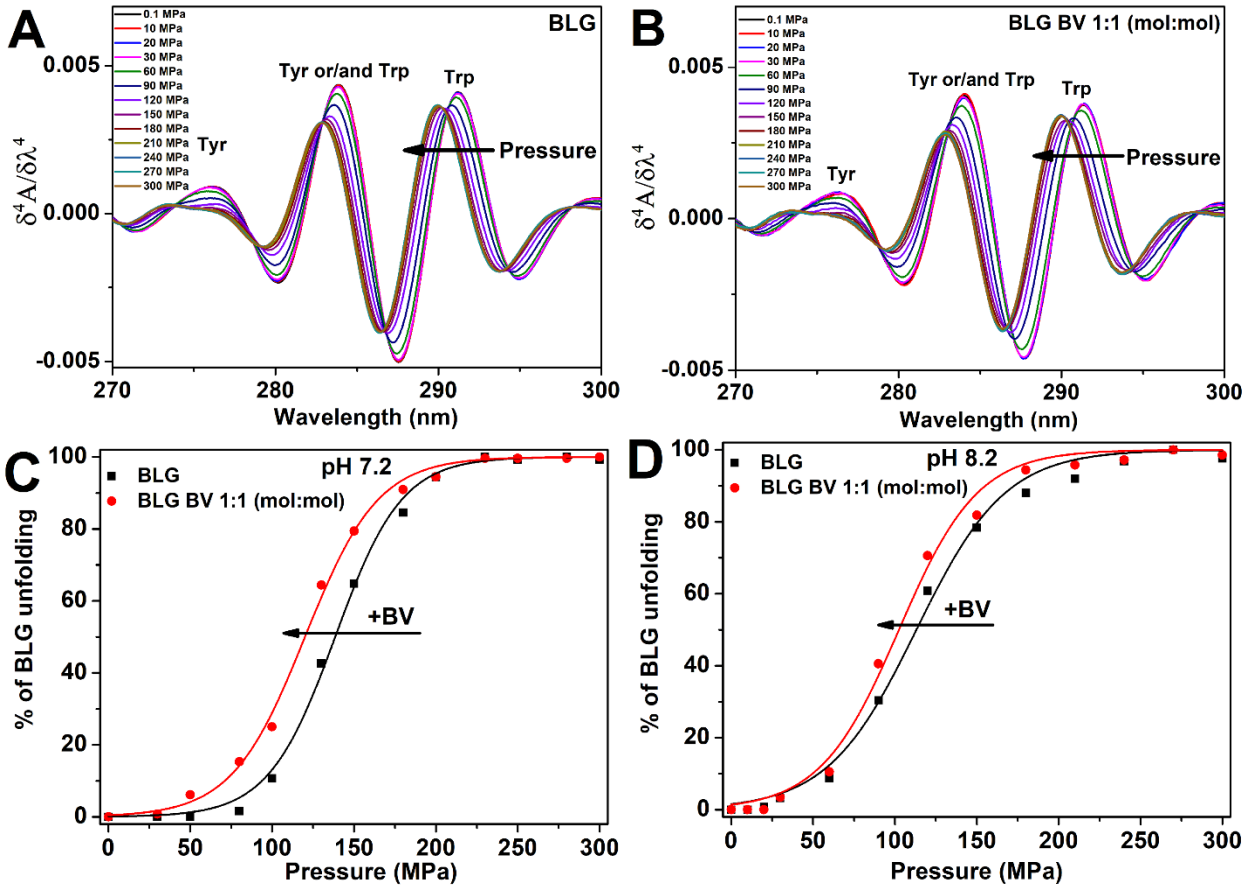

Figure 5. *4th derivative of in situ HP-UV absorption spectra of BLG (2 mg/mL) in the absence (**A**) or presence (**B**) of BV (molar ratio 1:1), at pH 8.2 (see Fig. S4, A-B, at pH 7.2). Percentage of unfolded BLG (Eq. 1, see text) as a function of pressure and the best fits (solid lines) calculated from Eq. 2 (see text), in absence or presence of BV at pH 7.2 (**C**) or 8.2 (**D**), obtained from the absorption spectra.*

The denaturation curves are well fitted by Eq. 2 (Fig. 5, C-D) but, since the HP denaturation of BLG is a pseudo-equilibrium (due to irreversible reactions discussed later), the only thermodynamic parameters that can be extracted are the apparent unfolding volume change ($_{app}\Delta V_u$) and the value of the half-denaturation pressure ($P_{1/2}$) listed in Table 2. The UV absorption measurements indicate destabilization effects of BV on the protein unfolding, without significant changes on ΔV_u. The destabilization effects of BV are more pronounced at pH 7.2 in comparison to pH 8.2. Additionally, for the unliganded BLG, an increase of pH from 7.2 to 8.2 decreases ΔV_u while, in the presence of BV, the pH-induced change of ΔV_u is much less pronounced (Fig 5, Table 2).

Table 2. *Thermodynamic parameters of pressure denaturation for BLG samples obtained from HP-UV absorption spectroscopy at 20°C.*

Sample	**pH**	$_{app}\Delta V_u$ **(mL/mol)**	$P_{1/2}$ **(MPa)**	$_{app}\Delta G_{P\,=\,0.1\,MPa}$ **(kJ/mol)**
BLG	7.2	-120 ± 7	139 ± 2	16.6 ± 0.9
	8.2	-90 ± 6	113 ± 2	10.1 ± 0.7

BLG-BV	7.2	-109 ± 6	120 ± 2	13.1 ± 0.6
	8.2	-101 ± 8	103 ± 3	10.4 ± 0.8

Note that it is not possible to test the effect of BV at the molar ratio of 1:4 since the absorption is too high and saturates the spectrophotometer detector.

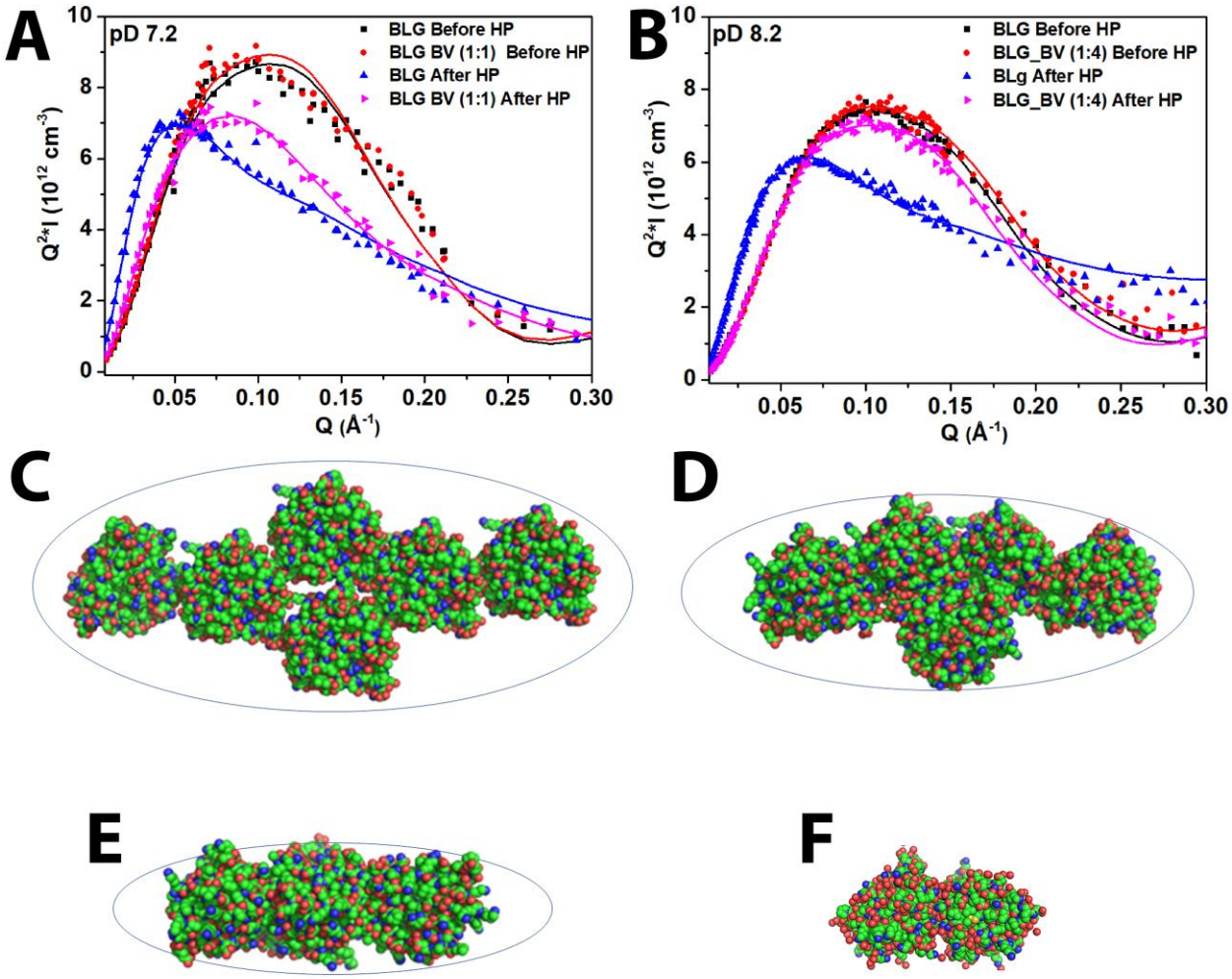

Figure 6*. (**A**) Kratky representation of BLG SANS intensities measured at pD 7.2 (**A**) and pD 8.2. (**B**) in quartz Hellma® cells before and after ~300 MPa HP treatment. The corresponding*

*coloured full lines represent the best fits to ellipsoid or cylinder models (see also Tables 1 and 2). (**C-F**) Ab initio shapes (top views) of BLG covalent oligomers after HP derived from the MASSHA models (Table 3): at pD 7.2, (**C**) BLG and (**E**) BLG-BV (1:1) complex and, at pD 8.2, (**D**) BLG and (**F**) BLG-BV (1:4) complex, the latter corresponding to the native dimer. Green, blue, and red spheres represent carbon, nitrogen, and oxygen atoms, respectively. For comparison, the ellipsoid shapes obtained from fits with SasView are superimposed to MASSHA model buildings.*

BLG refolding and oligomerization. The binding of BV slightly inhibits the covalent *in situ* oligomerization of BLG induced by HP: at 200-300 MPa, R_g, $I_{Q\to 0}$, and the length of the cylinder are slightly decreased compared to the protein without ligand, whereas the onsets are not significantly shifted by BV (Fig. 4). The release to the atmospheric pressure does not enable to recover a complete folded state for BLG, rather causes irreversible covalent oligomerization with a significant increase of both $I_{Q\to 0}$ and R_g (Table 3 and Fig. S5), as well as $D_{\max}$ obtained from the $P(r)$ calculation (Fig. S6 and Table S2), compared to samples before HP treatment (Tables 1 and S1). However, a partial globular shape is observed, as evidenced by the bell-shaped SANS curves in Kratky representation (Fig. 6, A-B). BLG could therefore be in a "molten globule" state with long term stability, as suggested previously in HP studies by fluorescence and circular dichroism.[3, 50]

In contrast, the addition of BV at molar ratio 1:1 at pH 7.2 significantly inhibits BLG oligomerization through inhibition of disulfide bond exchange, but without the ability to completely suppress it (Figs. 6A and S4A). Taking advantage of the better solubility of BV at higher pH values, we tested the effects of higher BV concentration (1:4 molar ratio) on HP-induced BLG oligomerization at pH 8.2. Adding four times more BV almost completely suppresses the

formation of BLG covalent oligomers by HP, Kratky curves before and after HP treatment being mostly superimposed (Figs. 6B and S4B, and Table 3 for $I_{Q\to 0}$ and R_g values), as observed with NEM-modified BLG.[51] We checked by SAXS that such partial or complete inhibition of oligomerization as a function of the BV:BLG molar ratio does not depend on whether the pH is 7.2 or 8.2 (Fig. S7).

Moreover, the solution structure of BLG:BV (1:4) is similar to the native structure of the unliganded BLG, as shown by the superimposition of the curves before and after pressure (Fig. 6B). It means that, at the SANS low resolution, BLG recovers its native 3D folding, despite the presence of the BV adduct, whose binding is irreversible, as well as possible disulfide redistribution.[52] As shown before, one BV ligand is bound *per* protein. Therefore, BLG still has two S-S bridges able to maintain a 3D structure.

Ellipsoid fitting and MASSHA rigid body *ab initio* modeling confirm that BV binding reduces significantly the size of the oligomers (Fig. 6, C-F, Table 3). The number of BLG "monomers" estimated by MASSHA simulations is consistent with the *MW* calculated from $I(0)$ in Guinier approximation, as well as with the ellipsoid or cylinder fitting (Table 3). A certain shift is nevertheless observed, which can be attributed both to the fact that MASSHA uses only whole building blocks and does not take into account a possible unfolding, even partial, of the latter (Fig. 6, Table 3).

Interestingly, HP treatment of unliganded BLG produces larger covalent oligomers at pH 7.2 compared to pH 8.2 (Fig. 6, C & D, Table 3). The smaller size of BLG oligomers at pH 8.2 may be ascribed to the fact that a relatively larger number of reactive intermediates with exposed free Cys residues is formed due to the dimer dissociation at that pH, even at the early stages of HP

treatment. This increases the probability of termination reactions, blocking reactive thiol groups and resulting in the formation of smaller disulfide-linked BLG oligomers.[47]

Table 3. *Fitting of SANS data from BLG samples after HP treatment (300 MPa), using Guinier approximation, triaxial ellipsoid modeling (SasView), or rigid body modeling (MASSHA, ATSAS). The parameters a, b, and c represent the minor, polar, and major equatorial radii of the ellipsoid, respectively.*

	Guinier approximation			**ellipsoid/cylinder* modeling**				**rigid-body modeling**		
after HP treatment	R_g **(Å)**	$I_{Q\to 0}$ **(cm^{-1})**	***MW*** **(kDa)**	***a*** **or** ***L*** **(Å)**	***b*** **or** ***r*** **(Å)**	***c*** **(Å)**	χ^2	**Number of BLG monomers**	MW_{app} **(kDa)**	χ^2
BLG (pD 7.2)	46 ± 3	1.15 ± 0.06	118 ± 5	9.6 ± 0.3	43 ± 1	103 ± 4	1.07	6	128.8	2.08
BLG-BV (1:1, pD 7.2)	32 ± 2	0.53 ± 0.02	54 ± 2	10.9 ± 0.4	22.5 ± 0.8	75 ± 2	0.53	3	55.2	1.41
BLG (pD 8.2)	40 ± 1	0.70 ± 0.02	72 ± 2	9.0 ± 0.4	33.4 ± 0.6	88 ± 2	0.30	5	73.6	1.85
BLG-BV (1:4, pD 8.2)*	23.4 ± 0.5	0.29 ± 0.01	29.7 ± 0.4	74 ± 1*	14.1 ± 0.2*	ND	0.30	ND		

**Fitted with the cylinder form factor instead of the ellipsoid model: L and r are the cylinder length and radius, respectively. ND: not determined since the curves for BLG:BV (1:4) at pD 8.2 and the one for the native BLG are almost superimposed (Fig. 6B).*

Moreover, high protein concentration (8 mg/mL) partially preserves BLG from a complete unfolding, whereas high pressures (250-300 MPa, 30°C) induce the formation of BLG covalent tetramers as described in our previous study.[3] Here, we observe protein oligomerization to a "trimeric" state because experiments were performed at a lower temperature (20°C) which could

decrease the extent of protein oligomerization. Therefore, even a moderate temperature change can significantly increase or decrease the extent of protein oligomerization at HP conditions.

Even the highest concentration of BV we used (molar ratio 4:1) does not completely suppress HP-induced covalent oligomerization of BLG, and BLG trimers around 48 kDa are still visible on the SDS-PAGE gel after HP treatment (Fig. 7B). SDS-PAGE in non-reducing conditions for BLG samples, at pD 7.2 or 8.2, confirms SANS results. BV strongly inhibits BLG covalent oligomerization (Fig. 7A), while the increase of BV relative concentration significantly enhances such effect (Fig. 7B).

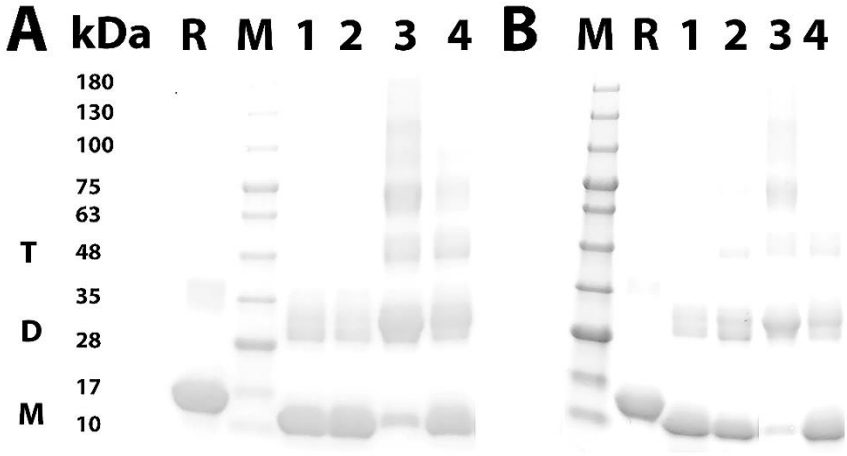

Figure 7. *SDS-PAGE (4-20% PAA gel) of (**A**) BLG samples (8 mg/mL or 435 μM) before or after HP-treatment at ~300 MPa at pD 7.2. BLG after HP treatment under reducing conditions (R), molecular size markers (M), BLG before HP in the absence (1) or presence (2) of 435 μM BV (BLG:BV 1:1), BLG after HP in the absence (3) or presence (4) of BV (1:1). T, D, and M denote BLG trimers, dimers, and monomers, respectively. (**B**) The same samples but at pD 8.2 and with BV concentration at 1,740 μM (BLG:BV 1:4). Same legend as in A.*

The present study shows that HP is a suitable tool for covalent modification of BLG using tetrapyrrole ligands such as BV, which could serve as a delivery system for bioactive pigments.[11, 53] In addition, BV ability to inhibit almost completely HP-induced oligomerization opens up new perspectives to modulate the techno-functional properties of BLG in food science, such as its colour, aggregation and/or allergenicity.[11, 53] Actually, it has been previously shown that covalent modification of BLG with polyphenols can decrease its allergenic potential.[54] Additionally, sulfhydryl-modified BLG exhibits a better foaming property, which is essential for the production of foam-based food products.[55] Furthermore, BV exhibits a high propensity towards photoisomerization when it is covalently attached to phytochromes, which makes it a potent tool in optogenetics.[21] Further studies are needed to comprehensively evaluate the effects of HP-induced binding of tetrapyrrole pigments, such as BV, on BLG properties.

CONCLUSION

We report that BV, a linear tetrapyrrole ligand, has significant effects on the structural changes of BLG induced by pressure, through covalent binding to BLG cysteines and SH/S-S rearrangements, as observed by MS/MS. Analytical fitting and *ab initio* modeling of SANS data show that the covalent binding of an excess of BV strongly inhibits BLG oligomerization upon the release of pressure and enables the protein to refold back toward its "native" 3D state, as shown at the SANS resolution. Surprisingly, this reversibility is not accompanied by a stabilization of the BLG-BV complex under pressure, compared to the protein without ligand, but rather by a slight destabilization - due to possible steric disturbances of the ligand on BLG structure - as observed by *in situ* HP-SANS and HP-UV absorption spectroscopy up to ~300 MPa. Our strategy opens up new possibilities for the structural determination of protein intermediates and oligomers using HP.

We reported recently, the effects on BLG structure under HP of two noncovalent ligands, retinol and resveratrol, whose affinity and binding sites are different[3]. Retinol, by binding the hydrophobic cavity of BLG, with high affinity, is able to significantly stabilize BLG under pressure, as well as to partly inhibit its oligomerization after pressure. In contrast, resveratrol, which binds at the surface of BLG, with low afffinity, has no significant effect on the protein structure under pressure. Together with these results, the present study highlights the effects of various bioactive molecules on BLG under pressure depending on their binding site, affinity, and chemical reactivity. We think our approach should be of benefit in future studies to choose suitable ligands to modulate the structural changes of BLG under pressure, and by extension to other proteins with similar properties, such as the presence of a hydrophobic cavity or of cysteines, free or involved in disulfide bonds.

DECLARATION OF INTEREST

The authors declare no competing interests.

AUTHOR CONTRIBUTIONS

SM, AB, and SC designed research; SM, BA, AH, AB, and SC conducted and/or performed pressure experiments; LS and DC performed and analyzed mass spectrometry experiments; SM, AB, and SC analyzed data; SM, AB, and SC wrote the paper.

ACKNOWLEDGMENTS

This work benefited from the facilities and expertise of the I2BC proteomic platform (Proteomic-Gif, SICaPS) supported by IBiSA, Ile-de-France Région, Plan Cancer, CNRS, and Paris-Sud University.

REFERENCES

1. Silva, J. L.; Foguel, D.; Royer, C. A., Pressure provides new insights into protein folding, dynamics and structure. *Trends Biochem Sci* **2001,** 26, (10), 612-8.

2. Royer, C. A., Revisiting volume changes in pressure-induced protein unfolding. *Biochim Biophys Acta* **2002,** 1595, (1-2), 201-9.

3. Minic, S.; Annighofer, B.; Helary, A.; Hamdane, D.; Hui Bon Hoa, G.; Loupiac, C.; Brulet, A.; Combet, S., Effect of Ligands on HP-Induced Unfolding and Oligomerization of beta-Lactoglobulin. *Biophys J* **2020,** 119, (11), 2262-2274.

4. Barba, F. J.; Terefe, N. S.; Buckow, R.; Knorr, D.; Orlien, V., New opportunities and perspectives of high pressure treatment to improve health and safety attributes of foods. A review. *Food Research International* **2015,** 77, 725-742.

5. Pottier, L.; Villamonte, G.; Lamballerie, M. d., Applications of high pressure for healthier foods. *Current Opinion in Food Science* **2017,** 16, 21-27.

6. Huang, H.-W.; Hsu, C.-P.; Yang, B. B.; Wang, C.-Y., Advances in the extraction of natural ingredients by high pressure extraction technology. *Trends in Food Science & Technology* **2013,** 33, (1), 54-62.

7. Norton, T.; Sun, D.-W., Recent Advances in the Use of High Pressure as an Effective Processing Technique in the Food Industry. *Food and Bioprocess Technology volume* **2008,** 1, 2-34.

8. Penchalaraju, M.; Shireesha, B., Preservation of foods by high-pressure processing-a review. *Indian Journal of Science and Technology* **2013,** 1, 30-38.

9. Zeece, M.; Huppertz, T.; Kelly, A., Effect of high-pressure treatment on in-vitro digestibility of β-lactoglobulin. *Innovative Food Science & Emerging Technologies* **2008,** 9, (1), 62-69.

10. Singh, H., Aspects of milk-protein-stabilised emulsions. *Food Hydrocolloids* **2011,** 25, (8), 1938-1944.

11. Minic, S.; Radomirovic, M.; Savkovic, N.; Radibratovic, M.; Mihailovic, J.; Vasovic, T.; Nikolic, M.; Milcic, M.; Stanic-Vucinic, D.; Cirkovic Velickovic, T., Covalent binding of food-derived blue pigment phycocyanobilin to bovine beta-lactoglobulin under physiological conditions. *Food Chem* **2018,** 269, 43-52.

12. Galazka, V. B.; Ledward, D. A.; Varley, J., High pressure processing of β-lactoglobulin and bovine serum albumin. In *Food colloids: Proteins, lipids and polysaccharides*, Dickinson, E.; Bergenståhl, B., Eds. The Royal Society of Chemistry: Cambridge, 1997.

13. Ball, G.; Shelton, M. J.; Walsh, B. J.; Hill, D. J.; Hosking, C. S.; Howden, M. E., A major continuous allergenic epitope of bovine beta-lactoglobulin recognized by human IgE binding. *Clin Exp Allergy* **1994,** 24, (8), 758-64.

14. Meng, X.; Bai, Y.; Gao, J.; Li, X.; Chen, H., Effects of high hydrostatic pressure on the structure and potential allergenicity of the major allergen bovine beta-lactoglobulin. *Food Chem* **2017,** 219, 290-296.

15. Brownlow, S.; Morais Cabral, J. H.; Cooper, R.; Flower, D. R.; Yewdall, S. J.; Polikarpov, I.; North, A. C.; Sawyer, L., Bovine beta-lactoglobulin at 1.8 A resolution--still an enigmatic lipocalin. *Structure* **1997,** 5, (4), 481-95.

16. Knudsen, J. C.; Otte, J.; Olsen, K.; Skibsted, L. H., Effect of high hydrostatic pressure on the conformation of b-lactoglobulin A as assessed by proteolytic peptide profiling. *International Dairy Journal* **2002,** 12, 791-803.

17. Funtenberger, S.; Dumay, E.; Cheftel, J. C., High Pressure Promotes b-Lactoglobulin Aggregation through SH/S-S Interchange Reactions. *Journal of Agricultural and Food Chemistry* **1997,** 45, 912-921.

18. Yang, J.; Powers, J. R.; Clark, S.; Dunker, A. K.; Swanson, B. G., Hydrophobic probe binding of beta-lactoglobulin in the native and molten globule state induced by high pressure as affected by pH, KIO(3) and N-ethylmaleimide. *J Agric Food Chem* **2002,** 50, (18), 5207-14.

19. Sassa, S., Why Heme Needs to Be Degraded to Iron, Biliverdin IXa, and Carbon Monoxide? *Antioxidants & Redox Signaling* **2004,** 6, (5), 819-824.

20. Narikawa, R.; Nakajima, T.; Aono, Y.; Fushimi, K.; Enomoto, G.; Ni Ni, W.; Itoh, S.; Sato, M.; Ikeuchi, M., A biliverdin-binding cyanobacteriochrome from the chlorophyll d-bearing cyanobacterium Acaryochloris marina. *Sci Rep* **2015,** 5, 7950.

21. Lamparter, T.; Carrascal, M.; Michael, N.; Martinez, E.; Rottwinkel, G.; Abian, J., The biliverdin chromophore binds covalently to a conserved cysteine residue in the N-terminus of Agrobacterium phytochrome Agp1. *Biochemistry* **2004,** 43, (12), 3659-69.

22. Sheehan, M. M.; Magaraci, M. S.; Kuznetsov, I. A.; Mancini, J. A.; Kodali, G.; Moser, C. C.; Dutton, P. L.; Chow, B. Y., Rational Construction of Compact de Novo-Designed Biliverdin-Binding Proteins. *Biochemistry* **2018,** 57, (49), 6752-6756.

23. Khrenova, M. G.; Kulakova, A. M.; Nemukhin, A. V., Competition between two cysteines in covalent binding of biliverdin to phytochrome domains. *Org Biomol Chem* **2018,** 16, (40), 7518-7529.

24. Lamparter, T.; Michael, N.; Caspani, O.; Miyata, T.; Shirai, K.; Inomata, K., Biliverdin binds covalently to agrobacterium phytochrome Agp1 via its ring A vinyl side chain. *J Biol Chem* **2003,** 278, (36), 33786-92.

25. Beuckmann, C. T.; Aoyagi, M.; Okazaki, I.; Hiroike, T.; Toh, H.; Hayaishi, O.; Urade, Y., Binding of biliverdin, bilirubin, and thyroid hormones to lipocalin-type prostaglandin D synthase. *Biochemistry* **1999,** 38, (25), 8006-13.

26. Zsila, F., A new ligand for an old lipocalin: induced circular dichroism spectra reveal binding of bilirubin to bovine beta-lactoglobulin. *FEBS Lett* **2003,** 539, (1-3), 85-90.

27. Fox, K.; Holsinger, V.; Posati, L.; Pallansch, M., Separation of β-lactoglobulin from other milk serum proteins by trichloroacetic acid. *Journal of Dairy Science* **1967,** 50, (9), 1363-1367.

28. Collini, M.; D'Alfonso, L.; Baldini, G., New insight on beta-lactoglobulin binding sites by 1-anilinonaphthalene-8-sulfonate fluorescence decay. *Protein Sci* **2000,** 9, (10), 1968-74.

29. Laemmli, U. K., Cleavage of structural proteins during the assembly of the head of bacteriophage T4. *Nature* **1970,** 227, (5259), 680-5.

30. Hoa, G.; Douzou, P.; Dahan, N.; Balny, C., High-Pressure Spectrometry at Subzero Temperatures *Analytical biochemistry* **1982,** 120, 125-135.

31. Dufour, E.; Hoa, G. H.; Haertle, T., High-pressure effects on beta-lactoglobulin interactions with ligands studied by fluorescence. *Biochim Biophys Acta* **1994,** 1206, (2), 166-72.

32. Lange, R.; Bee, N.; Mozhaev, V. V.; Frank, J., Fourth derivative UV-spectroscopy of proteins under high pressure II. Application to reversible structural changes. *European Biophysics Journal* **1996,** 24, 284-292.

33. Annighofer, B.; Helary, A.; Brulet, A.; Colas de la Noue, A.; Loupiac, C.; Combet, S., A high pressure cell using metallic windows to investigate the structure of molecular solutions up to 600 MPa by small-angle neutron scattering. *Rev Sci Instrum* **2019,** 90, (2), 025106.

34. Brulet, A.; Lairez, D.; Lapp, A.; Cotton, J. P., Improvement of data treatment in small-angle neutron scattering. *Journal of Applied Crystallography* **2007,** 40, 165-177.

35. Konarev, P. V.; Volkov, V. V.; Sokolova, A. V.; Koch, M. H. J.; Sverguna, D. I., PRIMUS: a Windows PC-based system for smallangle scattering data analysis. *Journal of Applied Crystallography* **2003,** 36, 1277-1282.

36. Guinier, A.; Fournet, G., *Small angle scattering of X-rays*. John Wiley & Sons, INC: New York, 1955; p 268.

37. Feigin, L. A.; Svergun, D. I., *Structure Analysis by Small-Angle X-Ray and Neutron Scattering*. Plenum: New York, 1987.

38. Konarev, P. V.; Petoukhova, M. V.; Sverguna, D. I., MASSHA-a graphics system for rigid-body modelling of macromolecular complexes against solution scattering data. *Journal of Applied Crystallography* **2001,** 34, 527-532.

39. Partanen, R.; Torkkeli, M.; Hellman, M.; Permi, P.; Serimaa, R.; Buchert, J.; Mattinen, M. L., Loosening of globular structure under alkaline pH affects accessibility of beta-lactoglobulin to tyrosinase-induced oxidation and subsequent cross-linking. *Enzyme Microb Technol* **2011,** 49, (2), 131-8.

40. Lowe, E. K.; Anema, S. G.; Bienvenue, A.; Boland, M. J.; Creamer, L. K.; Jimenez-Flores, R., Heat-induced redistribution of disulfide bonds in milk proteins. 2. Disulfide bonding patterns between bovine beta-lactoglobulin and kappa-casein. *J Agric Food Chem* **2004,** 52, (25), 7669-80.

41. Arciero, D. M.; Dallas, J. L.; Glazer, A. N., In vitro attachment of bilins to apophycocyanin. II. Determination of the structures of tryptic bilin peptides derived from the phycocyanobilin adduct. *J Biol Chem* **1988,** 263, (34), 18350-7.

42. Mercadante, D.; Melton, L. D.; Norris, G. E.; Loo, T. S.; Williams, M. A.; Dobson, R. C.; Jameson, G. B., Bovine beta-lactoglobulin is dimeric under imitative physiological conditions: dissociation equilibrium and rate constants over the pH range of 2.5-7.5. *Biophys J* **2012,** 103, (2), 303-12.

43. Anghel, L.; Rogachev, A.; Kuklin, A.; Erhan, R. V., beta-Lactoglobulin associative interactions: a small-angle scattering study. *Eur Biophys J* **2019,** 48, (3), 285-295.

44. Panick, G.; Malessa, R.; Winter, R., Differences between the pressure- and temperature-induced denaturation and aggregation of beta-lactoglobulin A, B, and AB monitored by FT-IR spectroscopy and small-angle X-ray scattering. *Biochemistry* **1999,** 38, (20), 6512-9.

45. Russo, D.; Ortore, M. G.; Spinozzi, F.; Mariani, P.; Loupiac, C.; Annighofer, B.; Paciaroni, A., The impact of high hydrostatic pressure on structure and dynamics of beta-lactoglobulin. *Biochim Biophys Acta* **2013,** 1830, (10), 4974-80.

46. Ortore, M. G.; Spinozzi, F.; Carsughi, F.; Mariani, P.; Bonetti, M.; Onori, G., High pressure small-angle neutron scattering study of the aggregation state of β-lactoglobulin in water and in water/ethylene-glycol solutions. *Chemical Physics Letters* **2006,** 418, (4-6), 342-346.

47. Hoffmann, M. A. M.; Mil, P. J. J. M. v., Heat-Induced Aggregation of b-Lactoglobulin: Role of the Free Thiol Group and Disulfide Bonds. *Journal of Agricultural and Food Chemistry* **1997,** 45, 2942-2948.

48. Ahmadi, S. K.; Moghadam, M. M.; Mokaberi, P.; Saberi, M. R.; Chamani, J., A comparison study of the interaction between βlactoglobulin and retinol at two different conditions:

spectroscopic and molecular modeling approaches. *Journal of Biomolecular Structure and Dynamics* **2014**.

49. Kolakowski, P.; Dumay, E.; Cheftel, J., Effects of high pressure and low temperature on β-lactoglobulin unfolding and aggregation. *Food Hydrocolloids* **2001,** 15, 215-232.

50. Yang, J.; Dunker, A. K.; Powers, J. R.; Clark, S.; Swanson, B. G., Beta-lactoglobulin molten globule induced by high pressure. *J Agric Food Chem* **2001,** 49, (7), 3236-43.

51. Tanaka, N.; Tsurui, Y.; Kobayashi, I.; Kunugi, S., Modification of the single unpaired sulfhydryl group of beta-lactoglobulin under high pressure and the role of intermolecular S-S exchange in the pressure denaturation [single SH of beta-lactoglobulin and pressure denaturation]. *Int J Biol Macromol* **1996,** 19, (1), 63-8.

52. Lowe, E. K.; Anema, S. G.; Bienvenue, A.; Boland, M. J.; Creamer, L. K.; Jimenez-Flores, R., Heat-induced redistribution of disulfide bonds in milk proteins. 2. Disulfide bonding patterns between bovine beta-lactoglobulin and kappa-casein. *J Agr Food Chem* **2004,** 52, (25), 7669-7680.

53. Radomirovic, M.; Minic, S.; Stanic-Vucinic, D.; Nikolic, M.; Van Haute, S.; Rajkovic, A.; Cirkovic Velickovic, T., Phycocyanobilin-modified β-lactoglobulin exhibits increased antioxidant properties and stability to digestion and heating. *Food Hydrocolloids* **2022,** 123.

54. Wu, X.; Lu, Y.; Xu, H.; Lin, D.; He, Z.; Wu, H.; Liu, L.; Wang, Z., Reducing the allergenic capacity of beta-lactoglobulin by covalent conjugation with dietary polyphenols. *Food Chem* **2018,** 256, 427-434.

55. Croguennec, T.; Renault, A.; Bouhallab, S.; Pezennec, S., Interfacial and foaming properties of sulfydryl-modified bovine beta-lactoglobulin. *J Colloid Interface Sci* **2006,** 302, (1), 32-9.